AT_2-Selective Angiotensin II Analogues Containing Tyrosine-Functionalized 5,5-Bicyclic Thiazabicycloalkane Dipeptide Mimetics

Petra Johannesson,[†] Máté Erdélyi,[†,‡] Gunnar Lindeberg,[†] Per-Anders Frändberg,[§] Fred Nyberg,[§] Anders Karlén,[†] and Anders Hallberg*,[†]

Department of Medicinal Chemistry, Uppsala University, BMC, Box 574, SE−751 23 Uppsala, Sweden, Department of Organic Chemistry, Uppsala University, BMC, Box 599, SE−751 24 Uppsala, Sweden, and Department of Biological Research on Drug Dependence, Uppsala University, BMC, Box 591, SE−751 24 Uppsala, Sweden

Received May 10, 2004

This paper reports the synthesis of two angiotensin II analogues with tyrosine-functionalized 5,5-bicyclic thiazabicycloalkane dipeptide mimetics replacing the Tyr[4]-Ile[5] residues. The preparation of these analogues relies on the synthesis and incorporation of an α,α-disubstituted chimeric amino acid derivative and on-resin bicyclization to a cysteine residue. The synthesized analogues both displayed high angiotensin AT_2/AT_1 receptor binding preferences and had AT_2 receptor affinities in the same low nanomolar range as angiotensin II itself. Conformational analysis, using experimental constraints derived from NMR studies, indicated that the Tyr[4] and His[6] residues in one of the angiotensin II analogues were in close proximity to each other.

Introduction

The linear octapeptide angiotensin II (Ang II, Chart 1) mediates its actions through binding to two pharmacologically distinct receptor subtypes, designated AT_1 and AT_2. Most of the well-known actions of Ang II, such as vasoconstriction, aldosterone release, sympathetic activation and cellular growth are mediated through the AT_1 receptor.[1−3] The function of the AT_2 receptor is less clear, but growing evidence supports its role in the regulation of antiproliferation processes, cellular differentiation, apoptosis and vascular relaxation.[4−8] The AT_2 receptor has recently attracted considerable interest as a new therapeutic target.

Although several different models of Ang II binding to the AT_1 receptor have been proposed,[9−18] it seems likely that the peptide adopts a reverse turn at the central Tyr[4] residue.[9−11,19−25] Understanding of the requirements for molecular recognition at the AT_2 receptor is more limited.[18,22,26−29] The introduction of monocyclic or bicyclic amino acid sequences into the 3−5 region of Ang II has been reported to result in analogues with retained AT_2 affinity, and it was postulated that Ang II binding at the AT_2 receptor might also involve a reverse turn in the Tyr[4] region of the molecule.[22,29] Recently an Ang II analogue with high AT_2 affinity and encompassing a γ-turn-like mimetic replacing amino acid residues 4−5 was also reported.[30]

It has been suggested that a reverse turn in a peptide could act as a recognition trigger in peptide−receptor interactions.[31] As a consequence, much time has been dedicated to the synthesis of structures that mimic or induce reverse turns.[32−41] The first generation of turn mimetics often suffered from the lack of side-chains, but during recent years many side-chain functionalized reverse turn mimetics have also been reported. One of the most successful examples of turn mimetics is seen in the family of thiazabicycloalkane dipeptide mimetics,[42−52] as represented here by structures **1**−**5** (Chart 2). The turn mimetics (**1**−**3**) were reported by Hruby and co-workers.[51,52] Johnson et al. prepared the type II′ β-turn mimetic **4**[46] and also compound **5**,[53] which

Chart 1. Structure of Angiotensin II

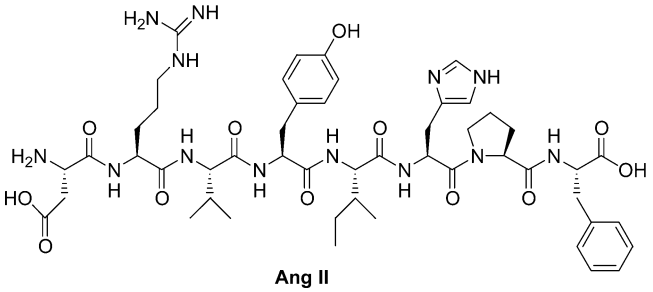

Chart 2. Structure of Thiazabicycloalkane Dipeptide Mimetics

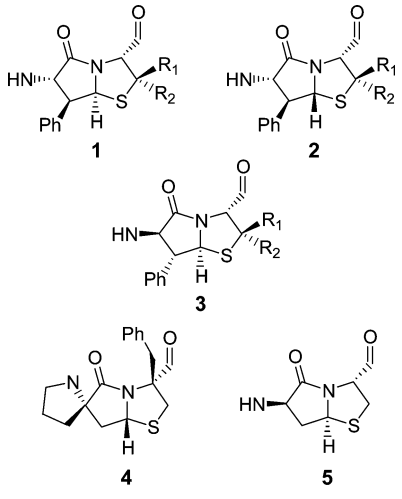

* Corresponding author. Telephone: +46 18 471 4284. Fax: +46 18 471 4976. E-mail: Anders.Hallberg@farmkem.uu.se.
† Department of Medicinal Chemistry.
‡ Department of Organic Chemistry.
§ Department of Biological Research on Drug Dependence.

10.1021/jm049651m CCC: $27.50
Published on Web 10/15/2004

Scheme 1. Synthetic Strategy Applied for the Preparation of the α,α-Disubstituted Building Block **13**[a]

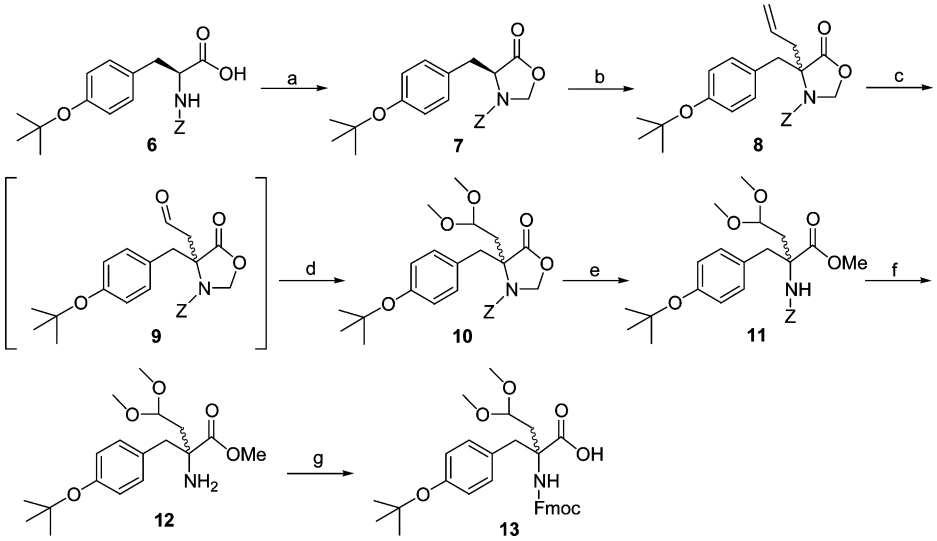

[a] Reagents and conditions: (a) Paraformaldehyde, benzene, reflux, 38% (95% based on consumed starting material); (b) KHMDS, allyl iodide, THF, −78 °C, 65%; (c) OsO_4, $NaIO_4$, H_2O/dioxane; (d) TsOH, MeOH, 61% over two steps, from compound **8**; (e) NaOMe, MeOH, reflux, 86%; (f) H_2, Pd/C, EtOH, 65 °C; (g) (i) KOH (aq), MeOH, reflux (ii) Fmoc-Cl, Na_2CO_3, H_2O/dioxane, 25% over two steps, from compound **11**.

was designed as a mimetic that could not achieve a β-turn conformation.

We have previously described a procedure for inducing spontaneous bicyclization which delivers tripeptide mimetic thiazabicycloalkanes after incorporation of a masked aldehyde building block and a cysteine residue into Ang II.[54,55] Upon liberation of the aldehydes by TFA, thiazabicycloalkanes spontaneously formed via connection of the side chains and a backbone nitrogen in the final step. This is in contrast to the most commonly used method for synthesis of thiazabicycloalkanes, which relies on intramolecular *N*-acylation as the final step.[42]

This paper reports the synthesis of Ang II analogues **16A** and **16B** (Scheme 2) which encompass tyrosine side-chain functionalized thiazabicycloalkane dipeptide mimetics replacing the Tyr^4 and Ile^5 residues, where a turn has been proposed to be important both for AT_1 and AT_2 receptor recognition. The preparation of these analogues relies on incorporation of the α,α-disubstituted chimeric amino acid derivative **13** (Scheme 1), and on-resin cyclization, employing methodology similar to that previously used by our group for formation of the corresponding tripeptide mimetics.[54,55] Both of the Ang II analogues exhibit high AT_2/AT_1 selectivity and a high affinity for the AT_2 receptor. We also present a conformational analysis, using experimental constraints derived from NMR studies of the two Ang II analogues in DMSO solution.

Results

Synthesis. The synthetic route to the α,α-disubstituted building block **13** is outlined in Scheme 1. Since the stereochemical outcome of the bridgehead carbon formed in the cyclization step was not obvious, and since we were interested in several of the subsequent potential diastereomeric target peptides, we desired access to both enantiomers of **13**. We therefore chose to use a racemic process of synthesis. The synthesis of the intermediate aldehyde **9** was based on a strategy outlined by Baldwin et al.[56] in their synthesis of the corresponding aldehyde derivative which was used to produce phenylalanine side-chain functionalized thiazabicycloalkanes, designated as γ-lactam analogues of β-lactam antibiotics.

The synthesis started with L-Z-Tyr(O^tBu)-OH (**6**). The oxazolidinone formation is usually achieved through reaction with paraformaldehyde and a catalytic amount of acid, such as *p*-toluenesulfonic acid, under azeotropic removal of water.[55,57] In this case, however, it was not possible to use acidic catalysis with *p*-toluenesulfonic acid, because of the presence of the acid-labile *tert*-butyl protecting group. The conversion to oxazolidinone **7** was sluggish in the absence of acid and resulted in a low yield of 38%. Fortunately, the starting material could be recovered and, based on its consumption, 95% yield was achieved.

Oxazolidinone **7** was deprotonated with potassium hexamethyldisilylamide (KHMDS), and the resulting enolate was alkylated with allyl iodide to form the racemic, quaternary-substituted amino acid derivative **8**. Oxidative cleavage of the double bond with sodium periodate and catalytic amounts of osmium tetroxide[58] afforded the aldehyde **9**, which was directly protected as the dimethyl acetal to give compound **10**.

The NMR spectra for compounds **7**, **8** and **10** were recorded at elevated temperatures in order to achieve signal coalescence of the rotameric mixtures. Nonetheless, it was necessary to report the NMR data for compound **10** as for a mixture of two rotamers (see Experimental Section).

Conversion to the primary amine **12** was performed by first cleaving the oxazolidinone with sodium methoxide in methanol and then removing the benzyloxycarbonyl group by catalytic hydrogenation. Cleavage of the oxazolidinone and benzyloxycarbonyl groups from compounds **10** and **11**, respectively, required higher temperatures than for deprotection of the corresponding monosubstituted compounds.[55] Reflux was also needed to effect hydrolysis of the methyl ester **12**. Finally, the amino function of the resulting zwitterion was directly

reacted with Fmoc-Cl to give the α,α-disubstituted building block **13**, which was incorporated into the pseudopeptide by standard Fmoc/*tert*-butyl solid-phase peptide synthesis (SPPS).

The SPPS incorporation and cyclization using the methods successfully employed in our earlier studies[54,55] met with limited success. Coupling of the quaternary substituted building block **13** was slow, as expected, but could be achieved by prolonging the reaction using (benzotriazol-1-yloxy)tripyrrolidinophosphonium hexafluorophosphate (PyBOP) activation. However, the next step, coupling of Fmoc-Val to the partially protected α,α-disubstituted amino acid residue, was unsuccessful. Several methods for proceeding were then evaluated, using small-scale experiments followed by cleavage and MS analysis. Activation with *O*-(7-azabenzotriazol-1-yl)-*N*,*N*,*N*′,*N*′-tetramethyluronium hexafluorophosphate (HATU) gave exclusively the tetramethylguanidine-modified starting peptide. Reaction with diisopropyl carbodiimide (DIC) and 1-hydroxy-7-azabenzotriazole (HOAt) produced an unidentified product as well as the starting material. Activation with PyBOP or use of Fmoc-Val-F or Fmoc-Val-OPfp resulted in only the starting peptide, although it was largely modified by monotritylation.

Steric hindrance, due to side-chain interactions and limited flexibility of the α,α-disubstituted residue, seemed to be the most likely explanation for the inaccessibility of the α-amino group for coupling with the carboxyl component, although a direct transfer of a trityl group to the α-amino function was also possible. In both cases, deprotection and on-resin cyclization before incorporation of Fmoc-Val was expected to facilitate the coupling reaction. Indeed, upon pretreatment of the peptide resin with 2% TFA in dichloromethane for 1.5 h, followed by coupling with Fmoc-Val-F[59,60] and removal of the Fmoc protecting group, the expected hexapeptide analogue was found to be the main product after cleavage. However, the reaction was still incomplete and the acid incubation of the Wang resin, because of the limited stability of the peptide−linker bond, was accompanied by an unacceptable loss of starting material. We therefore deemed it necessary to consider resins of higher acid stability.

Preliminary experiments with the acid stable-HYCRAM resin[61,62] were promising. We found, however, that Pd(0)-induced cleavage led to concomitant oxidation of methionine to the corresponding sulfoxide. Since our target peptide would also contain a thioaminal entity, the risk of oxidation forced us to abandon this approach.

Instead, we turned our attention to photolabile linkers. The use of the 4-ethyl-2-methoxy-5-nitrophenoxyacetyl based P-linker-2[63,64] attached to TentaGel S NH_2, although of low capacity, finally allowed synthesis, on-resin cyclization, and cleavage to proceed satisfactorily (Scheme 2).

The synthesis outlined in Scheme 2 afforded two main compounds with the expected mass and amino acid ratios. These two Ang II analogues, referred to as **16A** and **16B**, were each isolated in 5% yield after purification by RP-HPLC. Building block **13** was incorporated into the peptides as the racemate, and an additional asymmetric center of unknown configuration was created at the ring junction of the bicyclic system. Formation of Ang II analogues encompassing four different diastereomeric core structures is therefore possible. However, it seems that only two of them were formed in significant amounts.

Scheme 2. Incorporation of **13** into a Pseudopeptide Mimicking Angiotensin II and Its On-Resin Cyclization[a]

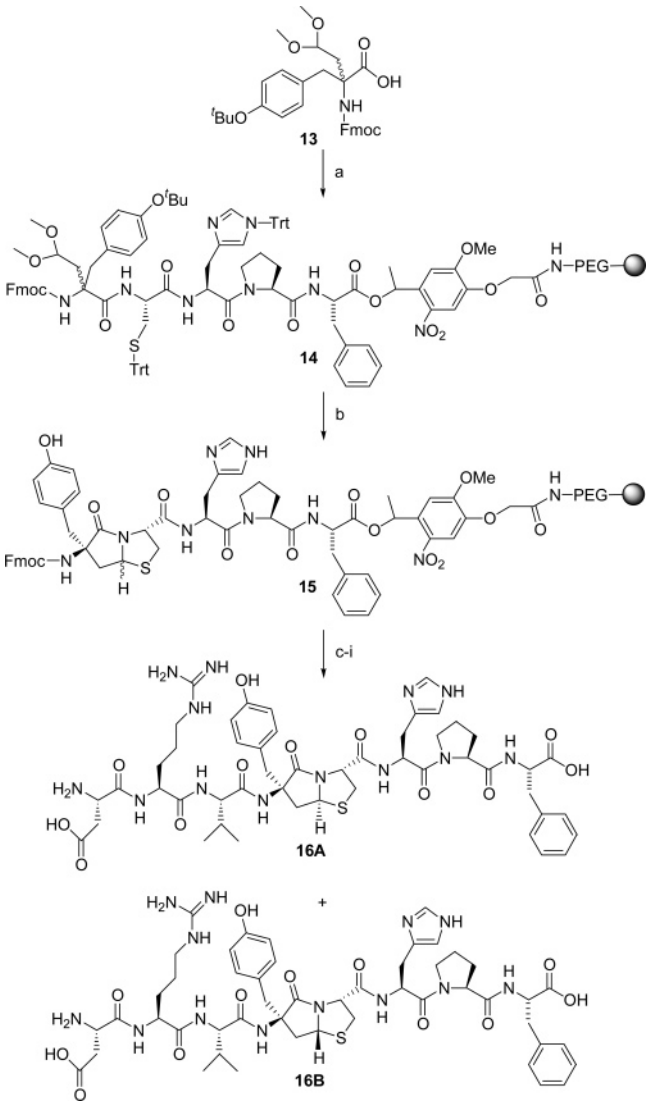

[a] Reagents and conditions: (a) Cys(Trt)-His(Trt)-Pro-Phe-P-linker-2-TentaGel, PyBOP, DIEA, DMF, overnight; (b) 95% TFA (aq); (c) piperidine, DMF; (d) (i) Fmoc-Val-F, DIEA, DMF, (ii) piperidine, DMF; (e) (i) Fmoc-Arg(Pbf), PyBOP, DIEA, DMF, (ii) piperidine, DMF; (f) (i) Fmoc-Asp(O^{t}Bu), PyBOP, DIEA, DMF, (ii) piperidine, DMF; (g) 95% TFA (aq), (h) $h\nu$ (350 nm), (i) purification by RP-HPLC.

Structural Characterization. The structural assignment of Ang II analogues **16A**and **16B** (Scheme 2), as well as determination of the stereochemistry of the bicyclic part of the molecules, was performed using data obtained from phase sensitive DQF−COSY,[65−67] gNOESY,[68,69] ROESY,[70] gTOCSY,[71] gHMQC[72,73] and gHMBC[74] NMR experiments. The observed NMR data was in good agreement with assignments of previous angiotensin analogues.[54,55] Selected ^{1}H NMR signals for **16A** and **16B** are given in Table 1 (for full spectral data and assignments, see Experimental Section). The diastereomeric Ang II analogues **16A** and **16B** both had an *R* configuration at the tyrosine side-chain functionalized carbon atom. **16B** also had an *R* configuration at

Table 1. Selected ^{1}H NMR Chemical Shifts for Ang II Analogues **16A** and **16B** (DMSO-d_6 solution, 25 °C)

compd	residue	$\Delta\delta/\Delta T^a$	NH	H-α	H-β	H-β'	H-γ	H-γ'	other
16A	Asp			4.11	2.78	2.63	-	-	
	Arg	2.9	8.58	4.36	1.64	1.51	1.51	1.51	NHϵ: 7.50 ($\Delta\delta/\Delta T^a$ = 2.6)
	Val	5.4	7.90	4.17	1.88	-	0.84	0.90	
	"Tyr"	6.7	8.29	-	2.95	2.90	-	-	ortho: 7.02; para: 6.70
	X[b]			-	2.67	2.33	3.95	-	
	Cys		-	4.79	3.19	3.21	-	-	
	His	1.0	7.58	4.83	3.07	2.85	-	-	H2: 9.30; H4: 7.28
	Pro		-	4.41	2.08	1.83	1.83	1.83	Hδ: 3.58; Hδ': 3.45
	Phe	4.3	8.37	4.47	3.04	2.95	-	-	Ar: 7.16−7.30
16B	Asp			4.12	2.79	2.63	-	-	
	Arg	3.6	8.68	4.39	1.67	1.52	1.52	1.43	NHϵ: 7.59 ($\Delta\delta/\Delta T^a$= 6.1)
	Val	5.9	7.95	4.26	1.96	-	0.81	0.83	
	"Tyr"	6.1	8.32	-	2.95	2.90	-	-	ortho: 6.99; para: 6.65
	X[b]			-	2.84	2.82	4.72	-	
	Cys		-	5.00	2.41	2.22	-	-	
	His	6.4	8.15	4.76	2.99	2.83	-	-	H2: 9.30; H4: 7.28
	Pro		-	4.41	2.04	1.81	1.78	1.81	Hδ: 3.47; Hδ': 3.58
	Phe	6.5	8.36	4.47	3.02	2.87	-	-	Ar: 7.16−7.30

[a] NMR temperature coefficients of NH chemical shifts (ppb/K). [b] X is used to denote the part derived from the aldehyde side chain of building block **13**, see Figure 1.

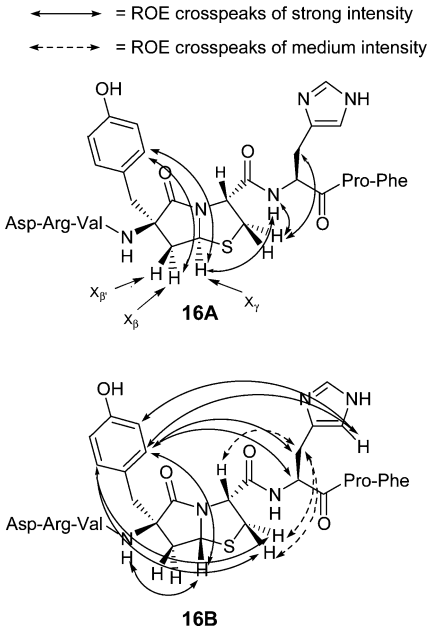

Figure 1. NOE information from Ang II analogues **16A** and **16B**.

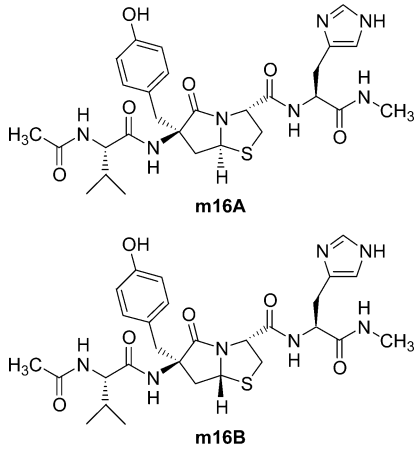

Figure 2. Model compounds used for conformational characterization.

the newly formed ring-junction carbon, while this ring-junction carbon had an *S* configuration in the epimeric **16A**. NOE information of Ang II analogues **16A** and **16B** is illustrated in Figure 1. For Ang II analogue **16B**, several ROESY cross-peaks indicated that the tyrosine and histidine side chains are within 5 Å proximity to each other in DMSO solution at room temperature. Low-temperature coefficients (Table 1) indicate that the histidine amide proton in Ang II analogue **16A** is hydrogen bonded and the arginine amide proton is in equilibrium between hydrogen bonded and non-hydrogen bonded states in DMSO solution at room temperature. For Ang II analogue **16B**, none of the amide protons seems to be hydrogen bonded under these conditions.

Molecular Modeling. To model the preferred conformations of Ang II analogues **16A** and **16B**, calculations for the blocked bicyclic tetrapeptides **m16A** and **m16B** (Figure 2) were performed using the experimental constraints derived from ROE cross-peaks (see Figure 1) observed in the ROESY spectra collected in DMSO-d_6 solution. Monte Carlo conformational searches combined with molecular mechanics energy minimization using the OPLS all atom force field were applied, and the GB/SA water solvation model[75] as implemented in the program Macromodel (version 7.0) was used.[76] The calculations resulted in 1154 low energy conformations for **m16A** and 695 conformations for **m16B** within 5 kcal/mol of the lowest energy minimum. The 20 lowest energy conformations of **m16A** and **m16B** are superimposed in Figure 3. The different stereochemistry in the bicyclic ring system enforces different ring geometries for **m16A** and **m16B**. This is also indicated by the computational analysis which shows that the side chains of Tyr^4 and His^6 in **m16B** are in close proximity. In contrast, this geometric arrangement is not preferred in the diastereomeric **m16A**. However, a few of the conformations identified for **m16A** adopt similar side-chain geometries to those seen with **m16B**. Furthermore, as indicated by Figure 3, both isomers of the thiazabicycloalkane dipeptide mimetics appear to mimic an extended backbone conformation.

In Vitro Binding Affinity. Ang II analogues **16A** and **16B** were evaluated in radioligand binding assays relying on displacement of [^{125}I]Ang II from AT_1 receptors in rat liver membranes[77] and from AT_2 receptors

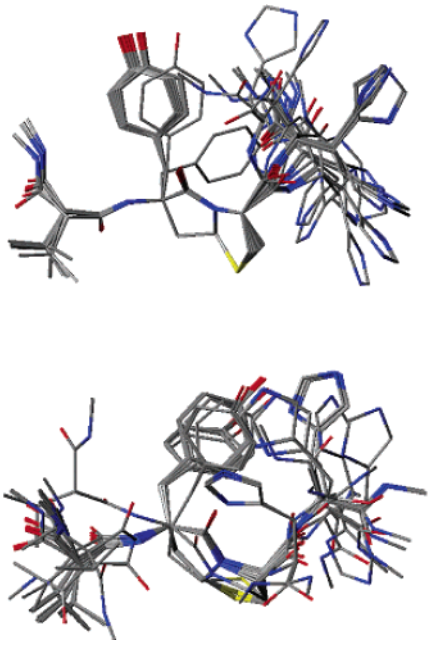

Figure 3. Overlaid backbones of the 20 lowest energy conformations of **m16A** (top) and **m16B** (bottom) from molecular modeling.

Table 2. In Vitro AT_1 and AT_2 Receptor Binding Affinities

compd	AT_1 (rat liver embranes) K_i (nM) ± SEM	AT_2 (pig uterus myometrium) K_i (nM) ± SEM
Ang II	1.1 ± 0.4	1.2 ± 0.4
[4-NH_2-Phe^6]AngII	>10000	1.4 ± 0.1
c[Hcy^{3,5}]Ang II	n.d.[a]	2.1 ± 0.1
losartan	1.9 ± 0.6	-
16A	>10000	1.0 ± 0.1
16B	>10000	3.7 ± 0.3

[a] n.d. = not determined.

in pig uterus membranes[78] (Table 2). Ang II, c[Hcy^{3,5}]-Ang II,[20] the highly AT_2 selective [4-NH_2−Phe^6]Ang II and the non-peptide AT_1-selective antagonist losartan were used as reference substances. Ang II analogues **16A** and **16B** both displayed high AT_2/AT_1 selectivity and bound with high affinities to the AT_2 receptor (affinity constants K_i 1.0 nM for **16A** and 3.7 nM for **16B**). Neither **16A** nor **16B** had any binding affinity to the AT_1 receptor; no K_i values below 10 μM were found.

Discussion

Building block **13** was incorporated into the peptides as the racemate. After SPPS and cyclization, two of the four possible diastereomeric target peptides were isolated. Both of the bicyclic Ang II analogues had the same stereochemistry as the naturally occurring L-tyrosine with respect to the tyrosine side-chain functionality. This may have been due to less effective SPPS incorporation of the *S*-enantiomer of **13** or to a lower tendency for appropriate folding and cyclization. According to the literature, the ring-junction hydrogen and the cysteine-derived carbonyl group in the diastereomer that is usually formed are on the same side of the thiazolidine ring.[42] Similar results were also obtained by Baldwin et al.[56] Their enantiomerically pure L-phenylalanine side-chain functionalized building block was reported to deliver the 5,5-bicyclic thiazabicycloalkane with stereochemistry corresponding only to **16A**. Our SPPS and on-resin cyclization, however, delivered epimer **16A** with an *S* configuration at the newly formed bridgehead carbon and epimer **16B** with the corresponding *R* configuration. It should be emphasized though that we cannot exclude that all four of the diastereomers had been formed in the reaction mixture, but that two of them escaped detection.

The thiazabicycloalkane **5** (Chart 2), with stereochemistry corresponding to that of **16A**, was designed as a dipeptide mimetic unable to adopt a β-turn conformation.[53] The crystal structure and conformational analysis of **3** (Chart 2), with the same stereochemistry as **16A**, indicated that this compound was also unlikely to adopt a turn conformation, with respect to reversal of the peptide backbone.[51] 5,5-Bicyclic thiazabicycloalkanes with stereochemistry corresponding to that of **16B** have to the best of our knowledge not yet been reported. Conformational analysis of carba-analogues with a carbon replacing the sulfur atom, however, indicated that these structures have poor reverse turn-inducing properties.[79] Although thiazabicycloalkanes in general have been successfully used as turn-inducing fragments, it seems that the 5,5-bicyclic dipeptide mimetics with the particular stereochemistry reported here, and with the incoming and outgoing peptide chain anti to each other, do not have reverse turn-inducing properties. This was also indicated by our conformational analysis of model tetrapeptides **m16A** and **m16B**, as can be seen from Figure 3.

Ang II analogues **16A** and **16B** both had high AT_2/AT_1 selectivity. They both displayed high affinity for the AT_2 receptor with K_i values of 1.0 and 3.7 nM, respectively, which is in the same range as that of Ang II itself (1.2 nM). In contrast to the current situation for the AT_1 receptor, relatively few investigations of the structure−activity relationships and conformation of Ang II binding to the AT_2 receptor have been reported.[2,18,22,27−30,80−82] Most of the binding affinity studies performed to date show that modifications of the linear peptides Ang II and [Sar^1]Ang II are well tolerated by the AT_2 receptor. Miura et al. reported that replacement with Ala at most positions in Ang II led to only minor decreases in AT_2 receptor affinity. The Arg^2, Tyr^4 and His^6 residues were most sensitive to substitution.[28] A recent Gly scan of Ang II showed that only substitution of Arg^2 resulted in significant reductions in AT_2 affinity.[83] Conformational analysis of AT_2 binding mono- and bicyclic Ang II analogues suggested the importance of a turn in the central Tyr^4 region of Ang II in its AT_2 binding conformation.[22,29] However, contrary to all previous suggestions, and as a result of photoaffinity labeling and site-directed mutagenesis experiments, Deraët et al. proposed that Ang II binds in an extended β-strand-like conformation at both the AT_1 and AT_2 receptors.[18] Our conformational analysis of Ang II analogues **16A** and **16B** indicates an extended backbone conformation in the Tyr^4-Ile^5 region of Ang II in solution. This is in accordance with the proposed model of Deraët et al. Furthermore the conformational analysis indicated that in analogue **16B** the Tyr^4 and His^6 side chains are in close proximity to each other.

For the AT_1 receptor, the Ang II aromatic side chains of the Tyr^4, His^6 and Phe^8 residues, as well as the *C*-terminal carboxylate, have been identified as the

pharmacophore groups.[2,84] The pharmacological evaluation showed that Ang II analogues **16A** and **16B** lacked affinity for the AT_1 receptor. Apparently these analogues cannot adopt a conformation that enables binding to this receptor, which fits with their inability to make a reverse turn around the central Tyr^4 residue, as has been proposed for Ang II in its AT_1-binding conformation.[9−11,19−25] Also the close proximity of the Tyr^4 and His^6 side chains in solution conformations of Ang II analogue **16B** do not fit proposed models of bioactive conformations such as that suggested by Nikiforovich et al.[10,11] Interestingly, the close spatial arrangement of the Tyr^4 and His^6 aromatic side chains does fit with the bioactive conformation of Ang II at the AT_1 receptor proposed by Moore and co-workers.[15] This model involves a charge relay system that requires clustering of the Tyr^4, His^6 and Phe^8 side chains. As is the case for our conformational analysis of Ang II analogues **16A** and **16B**, the model of Moore et al. is based on biophysical studies of Ang II and conformationally constrained Ang II analogues in solution.

Conclusion

The tyrosine derivative **13**, α-substituted with a masked aldehyde side chain, has been synthesized in seven steps from Z-Tyr(O^{t}Bu)-OH (**6**). Compound **13** was used in SPPS with the photolabile P-linker-2-TentaGel as solid support.[63,64] Upon acidic liberation of the aldehyde, on-resin cyclization occurred spontaneously, leading to formation of 5,5-bicyclic thiazabicycloalkane dipeptide mimetics substituted with a tyrosine side-chain.

The cyclization procedure was applied for the synthesis of two Ang II analogues containing the 5,5-bicyclic conformational constraint located in the important Tyr^4-Ile^5 region. The two constrained Ang II analogues exhibited high AT_2/AT_1 selectivity and an AT_2 binding affinity in the same range as for Ang II itself. Conformational analysis using experimental constraints derived from NMR studies supported the hypothesis of an extended backbone conformation in the Tyr^4-Ile^5 region. Furthermore, our conformational analysis indicated close proximity of the Tyr^4 and His^6 side chains in one of the AT_2-selective angiotensin II analogues.

Experimental Section

Chemistry. General Comments. ^{1}H and ^{13}C NMR spectra were recorded on a JEOL JNM-EX270 (^{1}H: 270.2 MHz, ^{13}C: 67.8 MHz), on a JEOL JNM-EX400 (^{1}H: 399.8 MHz, ^{13}C: 100.5 MHz), and on a Varian Inova 800 MHz (^{1}H: 799.9 MHz) spectrometer. The gNOESY spectrum (t_{mix} = 0.4 s) of the octapeptide **16A** was recorded on a Varian Unity 400 spectrometer operating at 400 MHz. Chemical shifts are reported as δ values (ppm), referenced indirectly to Me_4Si via the solvent residual signal. IR spectra were recorded on a Perkin-Elmer model 1605 FT-IR instrument, and for solids, a mounted Microfocus Beam Condenser with ZnSe lenses in a Diasqueeze Plus Diamond Compressor Cell (Graseby Specac Inc., Smyrna, U.S.A.) was used unless otherwise noted. IR values are reported as υ_{max} (cm^{-1}). Optical rotation was measured on a Perkin-Elmer Model 241 polarimeter. Melting points (uncorrected) were determined in open glass capillaries using a melting point microscope. Elemental analyses were performed by Mikro Kemi AB, Uppsala, Sweden. Flash column chromatography was performed using Merck silica gel 60 (40−63 μm). Thin-layer chromatography (TLC) was performed using aluminum sheets precoated with silica gel 60 F_{254} (0.2 mm, E. Merck). Chromatographic spots were visualized by UV and/or spraying with an ethanolic solution of ninhydrin (2%), followed by heating. Mass spectroscopy was carried out on an Applied Biosystems (Uppsala, Sweden) BIOION 20 plasma desorption mass spectrometer. Amino acid analyses and peptide content determinations were performed at the Department of Biochemistry, Biomedical center, Uppsala, Sweden, on 24 h hydrolyzates with an LKB 4151 alpha plus analyzer, using ninhydrin detection.

Materials. Z-L-Tyr(^{t}Bu)-OH (**6**) was isolated from the corresponding commercially available dicyclohexylamine salt by extraction. Fmoc-Val-F was prepared from Fmoc-Val-OH and cyanuric fluoride according to the literature.[59,60] Fmoc-Phe-Wang resin was obtained from Calbiochem-Novabiochem (Läufelfingen, Switzerland), and Boc-Phe-HYCRAM resin from Orpegen Pharma (Heidelberg, Germany). P-linker-2-TentaGel[63,64] was a gift from Doc. Eva Åkerblom, Department of Medicinal Chemistry, Uppsala University, BMC, Uppsala, Sweden. Amino acid derivatives and 2-(1*H*-benzotriazol-1-yl)-1,1,3,3-tetramethyluronium hexafluorophosphate (HBTU) were from Alexis Corp. (Läufelfingen, Switzerland), (benzotriazol-1-yloxy)tripyrrolidinophosphonium hexafluorophosphate (PyBOP) from Calbiochem-Novabiochem. DMF (purum) was purchased from Fluka Chemie GmbH (Buchs, Switzerland) and was used without further purification.

(4*S*)-3-(Benzyloxycarbonyl)-4-(4-*tert*-butoxyphenylmethyl)-1,3-oxazolidin-5-one (7). Z-L-Tyr(^{t}Bu)-OH (6) (28.3 g, 76.2 mmol) was dissolved in benzene (500 mL), and paraformaldehyde (95%) (6.86 g, 217 mmol) was added. The reaction mixture was immersed into a prewarmed oil bath and refluxed with azeotropic removal of water using a Dean−Stark apparatus for 24 h. Additional amounts of paraformaldehyde were added after 17 h (6.86 g, 217 mmol) and 20 h (6.86 g, 217 mmol). Most of the benzene was evaporated, and the residue was dissolved in EtOAc (500 mL) and washed with brine (150 mL). The organic phase was dried ($MgSO_4$) and evaporated. The residue was purified by flash column chromatography (gradient system: isohexane to isohexane/EtOAc 3:2) to afford recovered starting material (**6**) (17.0 g, 60%) and product (**7**) (11.0 g, 38% (95% based on consumed starting material)) as an oil: TLC R_f = 0.4 (isohexane/EtOAc 3:2); $[\alpha]_D$ = +189° (c = 0.99, 99% EtOH, 22 °C); ^{1}H NMR (acetone-d_6, 50 °C, 270.2 MHz) δ 1.26 (s, 9H, $C(CH_3)_3$), 3.04 (dd, J = 3.0, 13.2 Hz, 1H, CH_{2a}-Tyr), 3.27 (br dd, 1H, CH_{2b}-Tyr), 4.39 (br d, 1H, $NCH_{2a}O$), 4.54 (br dd, 1H, CH_2CH(N)-CO), 5.17 (br d, 1H, CH_{2a}-Z), 5.23 (br d, 1H, CH_{2b}-Z), 5.28 (d, J = 4.0 Hz, 1H, $NCH_{2b}O$), 6.82 (dm, J = 8.5 Hz, 2H, Ar-Tyr), 6.95 (dm, J = 8.5 Hz, 2H, Ar-Tyr), 7.26−7.44 (m, 5H, Ar-Z). ^{13}C NMR (acetone-d_6, 50 °C, 67.8 MHz) δ 29.7 ($C(CH_3)_3$), 36.2 (CH_2-Tyr), 57.7 (CH_2CH(N)-CO), 68.5 (CH_2-Z), 79.16 ($C(CH_3)_3$), 79.23 (NCH_2O), 125.2 (CH-Ar Tyr), 129.5, 129.6, 129.9 (CH-Ar Z), 131.2 (ipso Ar), 131.5 (CH Ar Tyr), 137.9 (ipso Ar), 153.7, 156.5 (ipso COC(CH_3)$_3$, CO Z), 173.0 (CH(N)CO); IR (KBr) 1795, 1685. Anal. ($C_{22}H_{25}NO_5$) C, H, N.

(4*R*,*S*)-3-(Benzyloxycarbonyl)-4-(4-*tert*-butoxyphenylmethyl)-4-[1-(2-propenyl)]-1,3-oxazolidin-5-one (8). Compound **7** (14.4 g, 37.5 mmol) was dissolved in dry THF (60 mL) in a dried three-necked flask fitted with a septum, a thermometer and a gas outlet for flushing with N_2. The solution was cooled to −78 °C. Potassium hexamethyldisilyl amide (KHMDS) as a 0.5 M toluene solution (187 mL, 93.5 mmol) was added slowly via a syringe, over 2 h, keeping the temperature below −70 °C. The temperature was monitored by a thermometer inside the flask. Thereafter allyl iodide (98%) (9.7 mL, 104 mmol) was added over 20 min, also via a syringe and keeping the temperature below −70 °C. The reaction mixture was stirred at −78 °C for 15 h and thereafter quenched by the addition of saturated aqueous NH_4Cl (250 mL). The quenched mixture was partitioned between diethyl ether (400 mL) and water (100 mL). The water phase was further extracted with diethyl ether (500 mL). The combined organic phases were dried ($MgSO_4$) and concentrated. The residue was purified by flash column chromatography (CH_2Cl_2) to give pure **8** (10.3 g, 65%) as a solid: mp 81−83 °C; TLC

R_f = 0.7 (1% MeOH in CH_2Cl_2); ^{1}H NMR (DMSO-d_6, 120 °C, 399.8 MHz) δ 1.29 (s, 9H, C(CH_3)$_3$), 2.61 (dd, J = 6.9, 14.0 Hz, 1H, CH_{2a}CH=CH_2), 2.98 (d, J = 13.8 Hz, CH_{2a}-Tyr), 3.06 (br dd, 1H, CH_{2b}CH=CH_2), 3.35 (br d, 1H, CH_{2b}-Tyr), 4.28 (d, J = 3.8 Hz, 1H, $NCH_{2a}O$), 5.05−5.33 (m, 5H, $NCH_{2b}O$, CH_2-Z, CH_2-CH=CH_2), 5.57−5.70 (m, 1H, CH_2CH=CH_2), 6.81 (m, 2H, Ar Tyr), 6.88 (m, 2H, Ar Tyr), 7.34−7.46 (m, 5H, Ar Z); ^{13}C NMR (DMSO-d_6, 120 °C, 67.8 MHz) δ 28.1 (C(CH_3)$_3$), 38.4, 39.0 (CH_2-CH=CH_2, CH_2-Tyr), 65.7, 66.3 (C(N)CO, CH_2-Z), 76.6 (NCH_2O), 77.3 (C(CH_3)$_3$), 119.3 (CH_2CH=CH_2), 122.5 (CH-Ar Tyr), 127.4, 127.5, 127.8 (CH-Ar Z), 128.5 (ipso Ar), 129.2 (CH-Ar Tyr), 130.5 (CH_2CH=CH_2), 135.5 (ipso Ar), 150.6, 154.2 (ipso COC-(CH_3)$_3$, CO Z,), 172.5 (C(N)CO); IR (solid) 1796, 1711. Anal. ($C_{25}H_{29}NO_5$) C, H, N.

(4*R*,*S*)-3-(Benzyloxycarbonyl)-4-(4-*tert*-butoxyphenylmethyl)-4-(2,2-dimethoxyethyl)-1,3-oxazolidin-5-one (10). To a solution of compound **8** (4.10 g, 9.68 mmol) in dioxane (23 mL) and water (4.8 mL) was added OsO_4 (4% in H_2O) (3.1 mL, 0.51 mmol). To this mixture was added $NaIO_4$ (6.21 mg, 29.0 mmol) in small portions, over 1.5 h, and the reaction mixture was stirred at room temperature for 22 h. Thereafter, the mixture was cooled to 0 °C, and the reaction was quenched by slowly adding saturated aqueous $NaHSO_3$ (70 mL). Stirring was continued at room temperature for 15 min. The reaction mixture was partitioned between diethyl ether (250 mL) and saturated aqueous $NaHSO_3$ (40 mL). The water phase was further extracted with diethyl ether (2 × 250 mL). The organic phases were combined and washed with saturated aqueous $NaHSO_3$ (130 mL). The organic phase was then dried ($MgSO_4$) and concentrated. The resulting crude aldehyde **9** was dissolved in MeOH (200 mL), *p*-toluenesulfonic acid (monohydrate, 98.5%) (1.31 g, 6.68 mmol) was added, and the mixture was stirred at room temperature for 15 h. Most of the solvent was evaporated, and the residue was partitioned between EtOAc (400 mL) and saturated aqueous $NaHCO_3$ (200 mL). The water phase was further extracted with diethyl ether (400 mL). The combined organic layers were dried ($MgSO_4$) and concentrated. Purification of the residue by flash column chromatography (isohexane/EtOAc 4:1) gave acetal **10** as an oil (2.78 g, 61%): TLC R_f = 0.55 (isohexane/EtOAc 7:3); NMR data are reported on a mixture of two conformers:^{1}H NMR (acetone-d_6, 50 °C, 270.2 MHz) δ 1.25 and 1.26 (2 × s, 9H, C(CH_3)$_3$), 2.19−2.31 (m, 1H, CH_{2a}CH(OMe)$_2$), 2.38−2.47 (m, 0.4H, CH_{2b}CH(OMe)$_2$), 2.56−2.65 (m, 0.6H, CH_{2b}CH(OMe)$_2$), 2.81−2.91 (m, 7.3 H, CH(OMe)$_2$ and CH_2-Tyr), 3.37−3.47 (m, 0.7H, CH_2-Tyr), 4.25−4.36 (m, 2H, CH(OMe)$_2$ and $NCH_{2a}O$), 4.92−5.02 (m, 1H, $NCH_{2b}O$), 5.07−5.16 (m, 0.7H, CH_2-Z), 5.26−5.35 (m, 1.3H, CH_2-Z), 6.70−6.90 (m, 4H, CH Ar Tyr), 7.28−7.56 (m, 5H, CH Ar Z); ^{13}C NMR (acetone-d_6, 50 °C, 67.8 MHz) δ 29.7 (C(CH_3)$_3$), 38.6, 39.9 (CH_2CH(OMe)$_2$), 41.4, 42.7 (CH_2-Tyr), 54.2, 54.5, 54.6, 54.7 (2 × OMe), 64.66, 64.74 (C(N)-CO), 68.1, 68.7 (CH_2-Z), 78.2, 78.5 (NCH_2O), 79.15, 79.17 (C(CH_3)$_3$), 103.2, 103.4 (CH(OMe)$_2$), 125.0 (CH-Ar Tyr), 129.57, 129.62, 129.9, 130.0, 130.4, 130.5, 130.7 (C ipso Ar and CH-Ar), 131.6 (CH-Ar Tyr), 137.6, 138.1 (C ipso Ar), 152.7, 153.4, 156.5, 156.6 (CO Z and ipso COC(CH_3)$_3$), 174.7, 175.1 (5); IR (neat) 1798, 1715; Anal. ($C_{26}H_{33}NO_7$) C, H, N.

(2*R*,*S*)-2-(Benzyloxycarbonylamino)-2-(4-*tert*-butoxyphenylmethyl)-4,4-dimethoxybutanoic Acid Methyl Ester (11). Compound **10** (1.15 g, 2.43 mmol) was dissolved in MeOH (40 mL) under N_2 atmosphere. Molecular sieves and NaOMe (95%) (395 mg, 6.95 mmol) were added. The reaction was refluxed for 2.5 h. 10% aqueous citric acid was added to pH 7, and most of the solvent was evaporated. The residue was partitioned between EtOAc (200 mL) and H_2O (100 mL). The water phase was further extracted with EtOAc (200 mL). The organic layers were combined, dried ($MgSO_4$) and evaporated. Purification of the residue by flash column chromatography (gradient system isohexane/EtOAc 17:3 to 3:1) afforded pure **11** (0.99 g, 86%) as a white solid: mp 74−76 °C; TLC R_f = 0.65 (isohexane/EtOAc 3:2); ^{1}H NMR ($CDCl_3$, 25 °C, 399.8 MHz) δ 1.31 (s, 9H, C(CH_3)$_3$), 2.26 (dd, J = 8.0, 14.0 Hz, 1H, CH_{2a}CH(OMe)$_2$), 2.79 (dd, J = 3.0, 14.0 Hz, 1H, CH_{2b}CH-(OMe)$_2$), 3.01 (d, J = 13.5 Hz, 1H, CH_{2a}-Tyr), 3.23 (s, 3H, CH-(OMe)$_2$), 3.28 (s, 3H, CH(OMe)$_2$), 3.51 (d, J = 13.5 Hz, 1H, CH_{2b}-Tyr), 3.70 (s, 3H, COOMe), 4.30 (dd, J = 3.0, 8.0 Hz, 1H, CH(OMe)$_2$), 5.07 (d, 1H, J = 12 Hz, CH_{2a}-Z), 5.21 (d, 1H, J = 12 Hz, CH_{2b}-Z), 5.82 (s, 1H, NH), 6.74−6.81 (m, 4H, CH Ar Tyr), 7.31−7.43 (m, 5H, CH Ar Z); ^{13}C NMR (acetone, 50 °C, 67.8 MHz) δ 28.7 (C(CH_3)$_3$), 38.9 (CH_2CH(OMe)$_2$), 40.3 (CH_2-Tyr), 52.3 (COOMe), 53.4 (CH(OMe)$_2$), 55.0 (CH(OMe)$_2$), 62.5 (C(NH)COOMe), 66.2 (CH_2-Z), 78.1 (C(CH_3)$_3$), 102.5 (CH-(OMe)$_2$), 123.6 (CH Ar Tyr), 128.0, 128.1, 128.4 (CH-Ar Z), 130.1 (CH-Ar Tyr), 130.2, 136.7 (ipso Ar), 154.17, 154.21 (CO Z and ipso COC(CH_3)$_3$), 172.7 (COOMe); IR (solid) 3394, 1741, 1709. Anal. ($C_{26}H_{35}NO_7$) C, H, N.

(2*R*,*S*)-2-Amino-2-(4-*tert*-butoxyphenylmethyl)-4,4-dimethoxybutanoic Acid Methyl Ester (12). Compound **11** (2.55 g, 5.38 mmol) and 10% Pd/C (284 mg, 267 μmol) were mixed in absolute EtOH (100 mL) and stirred under H_2 (1 atm), at 65 °C for 40 min. The mixture was filtered through Celite, and the Celite was washed with additional EtOH (300 mL). Concentration gave crude **12** (1.89 g) which could be used in the next step, without further purification. An analytical sample was prepared through purification by flash column chromatography (CH_2Cl_2/MeOH 9:1). White solid material: mp 55−56 °C; TLC R_f = 0.6 (5% MeOH in CH_2Cl_2); ^{1}H NMR ($CDCl_3$, 25 °C, 270.2 MHz) δ 1.32 (s, 9H, C(CH_3)$_3$), 1.96 (dd, J = 14.0, 5.5 Hz, 1H, CH_{2a}CH(OMe)$_2$), 2.05 (br s, 2H, NH_2), 2.29 (dd, J = 14.0, 5.5 Hz, 1H, CH_{2b}CH(OMe)$_2$), 2.77 (d, J = 13.5 Hz, 1H, CH_{2a}-Tyr), 3.09 (d, J = 13.5 Hz, 1H, CH_{2b}-Tyr), 3.30 (s, 3H, CH(OMe)$_2$), 3.32 (s, 3H, CH(OMe)$_2$), 3.67 (s, 3H, COOMe), 4.48 (t, J = 5.5 Hz, 1H, CH(OMe)$_2$), 6.89 (dm, J = 8.5 Hz, 2H, CH-Ar Tyr), 7.03 (dm, J = 8.5 Hz, 2H, CH-Ar Tyr); ^{13}C NMR ($CDCl_3$, 25 °C, 67.8 MHz) δ 28.8 (C(CH_3)$_3$), 42.4 (CH_2-CH(OMe)$_2$), 46.2 (CH_2-Tyr), 51.8 (COOMe), 53.3 (CH(OMe)$_2$), 53.4 (CH(OMe)$_2$), 60.1 (C(NH_2)COOMe), 78.2 (C(CH_3)$_3$), 102.4 (CH(OMe)$_2$), 123.9 (CH Ar), 130.4 (ipso Ar and CH-Ar, 2 C overlapping), 154.4 (ipso COC(CH_3)$_3$), 176.4 (COOMe); IR (solid) 3384, 3321, 1732. Anal. ($C_{18}H_{29}NO_5$) C, H, N.

(2*R*,*S*)-2-(4-*tert*-butoxyphenylmethyl)-2-[(9-fluorenylmethoxycarbonyl)- amino]-4,4-dimethoxybutanoic Acid (13). To compound **12** (1.00 g, 2.95 mmol) dissolved in MeOH (40 mL) was added 1 M aqueous KOH (7.4 mL, 7.4 mmol), and the mixture was refluxed for 3 h. 10% aqueous citric acid was added to pH 9, and the reaction mixture was concentrated to give a solid residue. This residue was dissolved in a mixture of 10% aqueous Na_2CO_3 (50 mL) and dioxane (25 mL) and cooled to 0 °C. Fmoc-Cl (97%, 1.91 g, 2.43 mmol) dissolved in dioxane (25 mL) was added dropwise, whereafter the reaction mixture was allowed to reach room temperature. The pH was kept around 10−11. Stirring at room temperature was continued for 68 h. 10% aqueous citric acid was added to pH 8−9, and the reaction mixture was washed with hexane (3 × 50 mL and 2 × 100 mL). Diethyl ether (200 mL) was added to the water phase, which was then acidified to pH 4 with 10% aqueous citric acid, under vigorous stirring. The phases were separated, and the water phase was further extracted with diethyl ether (2 × 200 mL). The combined organic layers were washed with water (2 × 100 mL), dried ($MgSO_4$) and concentrated to give the building block **13** (398 mg, 25% over two steps, from compound 11) as a white foam; TLC R_f = 0.35 (5% MeOH in CH_2Cl_2); ^{1}H NMR ($CDCl_3$, 25 °C, 270.2 MHz) δ 1.31 (s, 9H, C(CH_3)$_3$), 2.33 (dd, J = 14.0, 7.6 Hz, 1H, CH_{2a}CH-(OMe)$_2$), 2.70 (dd, J = 14.0, 3.8 Hz, 1H, CH_{2b}CH(OMe)$_2$), 3.12 (d, J = 13.5 Hz, 1H, CH_{2a}-Tyr), 3.28 (s, 3H, CH(OMe)$_2$), 3.33 (s, 3H, CH(OMe)$_2$), 3.49 (d, J = 13.5 Hz, 1H, CH_{2b}-Tyr), 4.26 (t, J = 6.5 Hz, 1H, CH-Fmoc), 4.36−4.47 (m, 2H, CH_{2a}-Fmoc and CH(OMe)$_2$), 4.56 (dd, J = 10.3, 6.5 Hz, 1H, CH_{2b}-Fmoc), 5.89 (s, 1H, NH), 6.83 (d, J = 7.6 Hz, 2H, CH-Ar), 6.94 (d, J = 7.6 Hz, 2H, CH-Ar), 7.28−7.46 (m, 4H, CH-Ar), 7.58−7.65 (m, 2H, CH-Ar), 7.78 (d, J = 7.6 Hz, 2H, CH-Ar); ^{13}C NMR ($CDCl_3$, 25 °C, 67.8 MHz) δ 28.8 (C(CH_3)$_3$), 38.7 (CH_2CH(OMe)$_2$), 40.2 (CH_2-Tyr), 47.3 (CH-Fmoc), 53.4 CH(OMe)$_2$), 54.7 CH(OMe)$_2$), 62.2 (C(NH)COOH), 66.3 (CH_2−Fmoc), 78.5 (C(CH_3)$_3$), 102.5 (CH(OMe)$_2$), 119.9, 123.8, 125.0, 127.1, 127.7 (CH-Ar), 130.1 (ipso Ar), 130.2 (CH-Ar), 141.3, 143.7, 143.8 (ipso Ar), 154.1,

154.6 (CO Fmoc and ipso *C*OC(CH_3)$_3$), 176.4 (COOH); IR (solid) 3408, 1713. Anal. ($C_{32}H_{37}NO_7 \cdot 1.75\ H_2O$) C, H, N.

H-Phe-P-linker-2-TentaGel. P-linker-2 resin (508 mg, ca. 90 μmol) was allowed to swell in 2.6 mL of dry CH_2Cl_2 in a 15 mL centrifuge tube. Fmoc-Phe-OH (132 mg, 340 μmol) was added and washed down with 2 × 2 mL CH_2Cl_2 followed by diisopropylcarbodiimide (53 μL, 340 μmol) and 4-pyrrolidinopyridine (7.1 mg, 48 μmol). The tube was capped, covered with Al-foil, and rotated at room temperature for 3 h. The resin was filtered off and washed with CH_2Cl_2 (5 × 7 mL) and DMF (5 × 7 mL). Ca. 10 mL 20% piperidine in DMF was then allowed to slowly pass through the polymer. Final removal of the Fmoc group was accomplished by treatment with a second 10-mL portion of the deprotection mixture in the capped filtration tube under rotation for 10 min. The resin was filtered, washed with DMF (5 × 7 mL), CH_2Cl_2 (5 × 7 mL) and MeOH (5 × 10 mL). The yield of the dried resin was 516 mg. The degree of substitution, as determined by amino acid analysis, was 0.18 mmol/g.

H-Cys(Trt)-His(Trt)-Pro-Phe-P-linker-2-TentaGel. To H-Phe-P-linker-2 resin (508 mg, 91 μmol) was added a solution of Fmoc-Pro-OH·H_2O (151 mg, 425 μmol) in DMF (2 mL) followed by HBTU (161 mg, 425 μmol) dissolved in DMF (2 mL), and DIEA (148 μl, 850 μmol). The contents of the covered filtration tube were mixed by rotation for 2h and then washed and deprotected as described above for the H-Phe-P-linker-2-TentaGel. The same procedure was used for the coupling of Fmoc-His(Trt)-OH (263 mg, 425 μmol) to yield 548 mg of the partially protected tripeptide resin. Part of the polymer (252 mg, 39.8 μmol) was transferred to a 5-mL disposable syringe equipped with a 20 μm polyethylene filter and reacted with Fmoc-Cys(Trt)-OH (116 mg, 198 μmol) and HBTU (75 mg, 198 μmol) in the presence of DIEA (69 μL, 396 μmol) essentially as described above for the other amino acids but with a coupling volume of 2 mL and with 3-mL washings. The dry, partially protected tetrapeptide resin weighed 267 mg. To a sample (3.6 mg) weighed into a transparent polypropylene Eppendorf tube was added MeOH (0.3 mL). The tube was capped and flushed with nitrogen and the suspension irradiated at 350 nm under stirring for 2 h.[63,64] LC-MS analysis showed the expected *m/z* values for the major component. No deletion peptides were detected.

Ang II Analogues 16A and 16B. Coupling of Building Block 13. In a 2-mL disposable syringe equipped with a polyethylene filter H-Cys(Trt)-His(Trt)-Pro-Phe-P-linker-2 resin (95.8 mg, 14.3 μmol) was reacted with building block **13** (9.2 mg, 16.8 μmol), PyBOP (8.7 mg, 16.8 μmol) and DIEA (7.3 μL, 42.0 μmol) in a total volume of 0.5 mL of DMF. The reaction was allowed to proceed under rotation in the dark for 18 h. The resin was filtered and washed with DMF (6 × 2 mL), MeOH (3 × 2 mL), CH_2Cl_2 (3 × 2 mL) and MeOH (6 × 2 mL) and dried in vacuo to yield 98.0 mg of compound **14**. A sample (4.1 mg) was cyclized and deprotected by treatment with 95% aq TFA for 1 h and then with 95% TFA containing 3% triethylsilane for 10 min in order to scavenge the trityl cations. After washing with ether, DMF and MeOH, the sample was cleaved by UV irradiation as described above. LC-MS analysis showed two isomers of the expected mass. However, since the incorporation was incomplete, the coupling was repeated with compound **13** (14.0 mg, 25.6 μmol), PyBOP (13.3 mg, 25.6 μmol) and DIEA (13.4 μL, 76.6 μmol) for 17 h. The resin was washed with DMF (6 × 2 mL), CH_2Cl_2 (6 × 2 mL) and MeOH (6 × 2 mL) and dried in vacuo. Yield of compound **14**: 95.9 mg. UV cleavage of an analytical sample (6.2 mg) now showed the reaction to be complete.

Cyclization Affording Compound 15. To remove the side-chain protecting groups and to induce the desired bicyclization, the remaining resin (**14**) (89.8 mg, 12.4 μmol) was treated with 95% aqueous TFA (2 × 2 mL, 2 × 30 min) and then with 95% aqueous TFA containing 50 μL of triethylsilane (2 mL, 10 min). The resin was filtered off and washed with CH_2Cl_2 (5 × 2 mL) and DMF (5 × 2 mL).

Coupling of Fmoc-Val-F. The Fmoc group was removed by reaction with three 2-mL portions of 20% piperidine in DMF (1, 3 and 10 min, respectively) and the polymer washed with DMF (6 × 2 mL). The resin above was reacted with Fmoc-Val-F (54.3 mg, 159 μmol) and DIEA (27.7 μL, 159 μmol) in 1 mL of DMF for 17.5 h and then washed and deprotected as described before. Cleavage and LC-MS (3.0 mg sample) confirmed that the coupling was complete.

Coupling of Fmoc-Arg(Pbf)-OH and Fmoc-Asp(O^{t}Bu)-OH. The peptide chain was further elongated by coupling with Fmoc-Arg(Pbf)-OH·diisopropyl ether (52.6 mg, 70.0 μmol), PyBOP (36.4 mg, 70.0 μmol) and DIEA (24.4 μL, 140.0 μmol) in 0.75 mL of DMF for 3 h. The resin was then washed and deprotected as described above. Fmoc-Asp(O^{t}Bu)-OH (28.8 mg, 70.0 μmol) was incorporated by the same procedure. After washing and removal of the Fmoc group, the resin was further washed with DMF (6 × 2 mL) and MeOH (6 × 2 mL) and dried to yield 84.8 mg. Side-chain deprotection was accomplished with TFA−H_2O−triethylsilane (90:5:5; 2 × 1.5 mL, 2 × 30 min). The resin was then washed with CH_2Cl_2 (6 × 2 mL), DMF (6 × 2 mL) and MeOH (6 × 2 mL) and dried. Yield: 82.2 mg.

Cleavage. The fully deprotected peptide resin was divided into three equal portions and transferred to 5-mL quartz tubes. After addition of 1.5 mL of MeOH, the tubes were capped with rubber septa and flushed with nitrogen for 2 min. The resin suspensions were then irradiated with UV light at 350 nm under stirring for 2 h. The polymer was removed by filtration through 0.45 μm centrifuge filters and further extracted with MeOH (0.5 mL) and 50% aqueous MeOH (2 × 0.5 mL). The combined filtrates were then evaporated to dryness in vacuo.

Purification. The residue after evaporation was dissolved in 2.5 mL of 0.1% aqueous TFA containing 10% MeCN and purified by two runs on a Vydac C18 (218TP) column (10 μm, 22 × 250 mm) using a gradient of MeCN in 0.1% aq TFA (5−55% MeCN in 75 min) at a flow rate of 3 mL/min and with detection by UV absorbance at 230 nm. The fractions were further analyzed by LC-MS using a Chromolith Performance RP-18e column (4.6 × 100 mm). Two major components were isolated, both showing the expected *m/z* values. **16A**: 0.65 mg (5.1%); LC-MS (MW 1059.7) 1060.6 ($M + H^+$), 531.0 ($M + 2H^+$)/2; amino acid analysis Asp, 0.98; Arg, 0.97; Val, 0.62; His, 1.03; Pro(+Cys), 1.22; Phe, 1.03 (81% peptide); ^{1}H NMR (DMSO-d_6, 25 °C, 400 MHz) δ 0.84 (d, J = 6.6 Hz, 3H, CH_3-Val), 0.90 (d, J = 7.0 Hz, 3H, CH_3-Val), 1.51 (m, 3H, H$_{\beta'}$-Arg, H$_{\gamma}$-Arg, H$_{\gamma'}$-Arg), 1.64 (m, 1H, H$_{\beta}$-Arg), 1.75−1.90 (m, 4H, H$_{\beta}$-Val, H$_{\beta'}$-Pro, H$_{\gamma}$-Pro, H$_{\gamma'}$-Pro), 2.08 (m, 1H, H$_{\beta}$-Pro), 2.33 (m, 1H, H$_{\beta'}$-X), 2.57−2.67 (m, 2H, H$_{\beta}$-X, H$_{\beta'}$-Asp), 2.77−2.98 (m, 5H, H$_{\beta}$-Asp, H$_{\beta'}$-His, H$_{\beta}$-Phe, H$_{\beta}$-Tyr, H$_{\beta'}$-Tyr), 3.00−3.12 (m, 4H, H$_{\beta'}$-Phe, H$_{\delta}$-Arg, H$_{\delta'}$-Arg, H$_{\beta}$-His), 3.16−3.25 (m, 2H, H$_{\beta}$-Cys, H$_{\beta'}$-Cys), 3.45 (m, 1H, H$_{\delta'}$-Pro), 3.58 (m, 1H, H$_{\delta}$-Pro), 3.95 (t, J = 7.1 Hz, H$_{\gamma}$-X), 4.11 (dd, J = 3.8, 8.6 Hz, 1H, H$_{\alpha}$-Asp), 4.17 (t, J = 8.2 Hz, 1H, H$_{\alpha}$-Val), 4.36 (m, 1H, H$_{\alpha}$-Arg), 4.40−4.50 (m, 2H, H$_{\alpha}$-Pro, H$_{\alpha}$-Phe), 4.79 (dd, 1H, J = 3.8, 6.6 Hz, H$_{\alpha}$-Cys), 4.83 (m, 1H, H$_{\alpha}$-His), 6.70 (AA′ part of AA′XX′, 2H, H$_{ortho}$-Tyr), 7.02 (XX′ part of AA′XX′, 2H, H$_{meta}$-Tyr), 7.28 (m, 6H, Phe, H-4 His), 7.50 (dd, J = 6.4 Hz, 1H, NH$_{\epsilon}$-Arg), 7.58 (d, J = 8.4 Hz, 1H, NH-His), 7.90 (d, J = 8.4 Hz, 1H, NH-Val), 8.29 (br s, 1H, NH-Tyr), 8.37 (d, J = 7.7 Hz, 1H, NH-Phe), 8.58 (d, J = 8.2 Hz, 1H, NH-Arg), 9.30 (br s, 1H, H-2 His). The histidine amide NH is hydrogen bonded, the Arg-NH is in exchange between H-bonded and non H-bonded states in DMSO solution at 25 °C. **16B**: 0.67 mg (5.3%); LC-MS 1060.6 ($M + H^+$), 531.0 ($M + 2H^+$)/2; amino acid analysis Asp, 0.97; Arg, 0.97; Val, 0.90; His, 1.03; Pro(+Cys), 1.12; Phe, 1.03 (84% peptide); ^{1}H NMR (DMSO-d_6, 25 °C, 400 MHz): δ 0.81 (d, J = 7.0 Hz, 3H, CH_3-Val), 0.83 (d, J = 7.0 Hz, 3H, CH_3-Val), 1.43 (m, 1H, H$_{\gamma'}$-Arg), 1.52 (m, 2H, H$_{\beta'}$-Arg, H$_{\gamma}$-Arg), 1.67 (m, 1H, H$_{\beta}$-Arg), 1.78 (m, 1H, H$_{\gamma}$-Pro), 1.81 (m, 2H, H$_{\beta'}$-Pro, H$_{\gamma'}$-Pro), 1.96 (dh, J = 7.0, 7.3 Hz, 1H, H$_{\beta}$-Val), 2.04 (m, 1H, H$_{\beta}$-Pro), 2.22 (dd, J = 4.0, 14.3 Hz, 1H, H$_{\beta'}$-Cys), 2.41 (dd, J = 7.0, 14.3 Hz, 1H, H$_{\beta}$-Cys), 2.63 (dd, J = 9.0, 18.1 Hz, 1H, H$_{\beta'}$-Asp), 2.79 (dd, J = 3.3, 18.1 Hz, 1H, H$_{\beta}$-Asp), 2.83−2.90 (m, 6H, H$_{\beta}$-X, H$_{\beta'}$-His, H$_{\beta'}$-X, H$_{\beta'}$-Phe, H$_{\beta}$-His, H$_{\beta'}$-Tyr), 2.98−3.10 (4H, m, H$_{\beta}$-Tyr, H$_{\beta}$-Phe, H$_{\delta}$-Arg, H$_{\delta'}$-Arg), 3.47 (m, 1H, H$_{\delta'}$-Pro), 3.58 (m, 1H, H$_{\delta}$-Pro), 4.12 (dd, J = 3.7, 8.4 Hz, 1H, H$_{\alpha}$-Asp), 4.26 (dd, J = 7.3,

8.8 Hz, 1H, H_α-Val), 4.37−4.48 (m, 3H, H_α-Arg, H_α-Pro, H_α-Phe), 4.72 (d, J = 3.2, 8.0 Hz, 1H, H_γ-X), 4.76 (dd, J = 5.6, 8.0 Hz, 1H, H_α-His), 5.00 (dd, J = 4.0, 7.0 Hz, 1H, H_α-Cys), 6.65 (AA′XX′, 2H, H_{ortho}-Tyr), 6.99 (AA′XX′, 2H, H_{meta}-Tyr), 7.16−7.30 (m, 5H, Phe), 7.28 (br s, 1H, H-4 His), 7.59 (t, J = 5.8 Hz, 1H, NH_ϵ-Arg), 7.95 (d, J = 8.8 Hz, 1H, NH-Val), 8.15 (d, J = 9.5 Hz, 1H, NH-His), 8.32 (br s, 1H, NH-Tyr), 8.36 (d, J = 7.3 Hz, 1H, NH-Phe), 8.68 (d, J = 7.7 Hz, 1H, NH-Arg), 9.30 (br s, 1H, H-2 His). None of the amide NH's are hydrogen bonded in the DMSO solution of this diastereomer at 25 °C. X is used to denote the part derived from the aldehyde side-chain of building block **13**, see Figure 1. The yields are corrected for peptide content.

Molecular Modeling. The conformational predictions of **m16A** and **m16B** were performed using the OPLS all atom force field as implemented in the program Macromodel 7.0.[76] The General Born Solvent Accessible (GB/SA) surface area method developed by Still[75] was used in all calculations. The number of torsion angles allowed to vary simultaneously during each Monte Carlo step ranged from 1 to $n - 1$, where n equals the total number of rotatable bonds. Amide bonds where fixed in the trans configuration. Conformational constraints derived from ROESY cross-peaks were introduced using the CDIS command (5 Å ± 1.5 Å) as implemented in Macromodel 7.0. For the conformational search 10000 Monte Carlo step runs were performed, and those conformations within 5 kcal/mol of the lowest energy minimum were kept. In the subsequent minimization a maximum of 40000 steps of PR conjugate gradient (PRCG) minimization resulted in 1154 and 695 fully converged structures for **m16A** and **m16B**, respectively.

Rat Liver Membrane AT_1 Receptor Binding Assay. Rat liver membranes were prepared according to the method of Dudley et al.[77] Binding of [^{125}I]Ang II to membranes was conducted in a final volume of 0.5 mL of 50 mM Tris-HCl (pH 7.4), supplemented with 100 mM NaCl, 10 mM $MgCl_2$, 1 mM EDTA, 0.025% bacitracin, 10 μM leupeptine, 10 μM bestatine, 10 μM pestatine A, 0.2% BSA and containing rat liver homogenate corresponding to 5 mg of the original tissue weight, [^{125}I]Ang II (80000 cpm, 36 pM), and variable concentrations of test substance. Samples were incubated at 25 °C for 90 min, and binding was terminated by filtration through Whatman GF/B glass-fiber filter sheets, using a Brandel cell harvester. The filters were washed with 4 × 2 mL of ice cold 50 mM Tris-HCl (pH 7.4) and transferred to tubes. The radioactivity was measured in a gamma counter. The characteristics of the Ang II binding AT_1 receptor was determined by using eight different concentrations (0.03−5 nM) of the labeled [^{125}I]Ang II. Nonspecific binding was determined in the presence of 1 μM Ang II. The specific binding was determined by subtracting the nonspecific binding from the total bound [^{125}I]Ang II. The dissociation constant (K_d = 0.8 ± 0.1 nM) was determined by Scatchard analysis of data obtained with Ang II using GraFit (Erithacus Software, UK). All experiments were performed in triplicates and were repeated at least three times. K_i values were calculated using the Cheng−Prusoff equation.

Porcine (Pig) Myometrial Membrane AT_2 Receptor Binding Assay. Myometrial membranes were prepared from porcine uteri according to the method of Nielsen et al.[78] Potential interference by binding to AT_1 receptors was blocked by addition of 1 μM losartan. Binding of [^{125}I]Ang II to membranes was conducted in a final volume of 0.5 mL of 50 mM Tris-HCl (pH 7.4), supplemented with 100 mM NaCl, 10 mM $MgCl_2$, 1 mM EDTA, 0.025% bacitracin, 10 μM leupeptine, 10 μM bestatine, 10 μM pestatine A, 0.2% BSA and containing homogenate corresponding to 10 mg of the original tissue weight, [^{125}I]Ang II (80000 cpm, 36 pM), and variable concentrations of test substance. Samples were incubated at 25 °C for 90 min, and binding was terminated by filtration through Whatman GF/B glass-fiber filter sheets, using a Brandel cell harvester. The filters were washed with 4 × 2 mL of ice cold 50 mM Tris-HCl (pH 7.4) and transferred to tubes. The radioactivity was measured in a gamma counter. The characteristics of the Ang II binding AT_2 receptor was determined by using six different concentrations (0.03−5 nM) of the labeled [^{125}I]Ang II. Nonspecific binding was determined in the presence of 1 μM Ang II. The specific binding was determined by subtracting the nonspecific binding from the total bound [^{125}I]-Ang II. The dissociation constant (K_d = 1.6 ± 0.2 nM) was determined by Scatchard analysis of data obtained with Ang II using GraFit (Erithacus Software, UK). The binding data were best fitted with a one-site fit. All experiments were performed in triplicates and were repeated three times except for 16B that were performed in duplicates. K_i values were calculated using the Cheng−Prusoff equation.

Acknowledgment. We thank Adolf Gogoll, Department of Organic Chemistry, Uppsala University, Uppsala, Sweden, for valuable advice concerning the NMR spectra of Ang II analogues **16A** and **16B**. The Swedish NMR Centre (Patrik Jarvoll), at Gothenburg University, Sweden, is gratefully acknowledged for use of a Varian Unity 800 spectrometer. We also thank Milad Botros, Department of Biological Research on Drug Dependence, Uppsala University, Sweden, for skillful in vitro binding experiments, and the Swedish Foundation for Strategic Research (SSF) for financial support.

References

(1) Timmermans, P. B.; Wong, P. C.; Chiu, A. T.; Herblin, W. F.; Benfield, P.; Carini, D. J.; Lee, R. J.; Wexler, R. R.; Saye, J. A.; Smith, R. D. Angiotensin II Receptors and Angiotensin II Receptor Antagonists. *Pharmacol. Rev.* **1993**, *45*, 205−251.
(2) De Gasparo, M.; Catt, K. J.; Inagami, T.; Wright, J. W.; Unger, T. International Union of Pharmacology. XXIII. The Angiotensin II Receptors. *Pharmacol. Rev.* **2000**, *52*, 415−472.
(3) Kaschina, E.; Unger, T. Angiotensin AT_1/AT_2 Receptors: Regulation, Signaling and Function. *Blood Pressure* **2003**, *12*, 70−88.
(4) Horiuchi, M. Functional Aspects of Angiotensin Type 2 Receptor. *Adv. Exp. Med. Biol.* **1996**, *396*, 217−224.
(5) Laflamme, L.; De Gasparo, M.; Gallo, J.-M.; Payet, M. D.; Gallo-Payet, N. Angiotensin II Induction of Neurite Outgrowth by AT_2 Receptors in NG108−15 Cells. − Effect Counteracted by the AT_1 receptors. *J. Biol. Chem.* **1996**, *271*, 22729−22735.
(6) Csikos, T.; Chung, O.; Unger, T. Receptors and Their Classification: Focus on Angiotensin II and the AT_2 Receptor. *J. Hum. Hypertens.* **1998**, *12*, 311−318.
(7) Gendron, L.; Oligny, J.-F.; Payet, M. D.; Gallo-Payet, N. Cyclic AMP−Independent Involvement of Rap1/B−Raf in the Angiotensin II AT_2 Receptor Signaling Pathway in NG108−15 Cells. *J. Biol. Chem.* **2003**, *278*, 3606−3614.
(8) Widdop, R. E.; Jones, E. S.; Hannan, R. E.; Gaspari, T. A. Angiotensin AT_2 Receptors: Cardiovascular Hope or Hype? *Br. J. Pharmacol.* **2003**, *140*, 809−824.
(9) Samanen, J. M.; Peishoff, C. E.; Keenan, R. M.; Weinstock, J. Refinement of a Molecular Model of Angiotensin II (AII) Employed in the Discovery of Potent Nonpeptide Antagonists. *Bioorg. Med. Chem. Lett.* **1993**, *3*, 909−914.
(10) Nikiforovich, G. V.; Marshall, G. R. Three-Dimensional Recognition Requirements for Angiotensin Agonists: A Novel Solution for an Old Problem. *Biochem. Biophys. Res. Commun.* **1993**, *195*, 222−228.
(11) Nikiforovich, G. V.; Kao, J. L.-F.; Plucinska, K.; Zhang, W. J.; Marshall, G. R. Conformational Analysis of Two Cyclic Analogues of Angiotensin: Implications for the Biologically Active Conformation. *Biochemistry* **1994**, *33*, 3591−3598.
(12) Joseph, M.-P.; Maigret, B.; Scheraga, H. A. Proposals for the Angiotensin II Receptor-Bound Conformation by Comparative Computer Modeling of AII and Cyclic Analogs. *Int. J. Pept. Protein Res.* **1995**, *46*, 514−526.
(13) Balodis, J.; Golbraikh, A. Conformational Analysis of Cyclic Angiotensin II Analogues. *Lett. Pept. Sci.* **1996**, *3*, 195−199.
(14) Carpenter, K. A.; Wilkes, B. C.; Schiller, P. W. The Octapeptide Angiotensin II Adopts a Well-Defined Structure in a Phospholipid Environment. *Eur. J. Biochem.* **1998**, *251*, 448−453.
(15) Matsoukas, J. M.; Polevaya, L.; Ancans, J.; Mavromoustakos, T.; Kolocouris, A.; Roumelioti, P.; Vlahakos, D. V.; Yamdagni, R.; Wu, Q.; Moore, G. J. The Design and Synthesis of a Potent Angiotensin II Cyclic Analogue Confirms the Ring Cluster Receptor Conformation of the Hormone Angiotensin II. *Bioorg. Med. Chem.* **2000**, *8*, 1−10.
(16) Polevaya, L.; Mavromoustakos, T.; Zoumboulakis, P.; Grdadolnik, S. G.; Roumelioti, P.; Giatas, N.; Mutule, I.; Keivish, T.; Vlahakos, D. V.; Iliodromitis, E. K.; Kremastinos, D. T.; Matsoukas, J. Synthesis and Study of a Cyclic Angiotensin II

Antagonist Analogue Reveals the Role of π^*-π^* Interactions in the C-terminal Aromatic Residue for Agonist Activity and Its Structure Resemblance with AT_1 Non-peptide Antagonists. *Bioorg. Med. Chem.* **2001**, *9*, 1639−1647.
(17) Boucard, A. A.; Wilkes, B. C.; Laporte, S. A.; Escher, E.; Guillemette, G.; Leduc, R. Photolabeling Identifies Position 172 of the Human AT_1 Receptor as a Ligand Contact Point: Receptor-Bound Angiotensin II Adopts an Extended Structure. *Biochemistry* **2000**, *39*, 9662−9670.
(18) Deraët, M.; Rihakova, L.; Boucard, A.; Perodin, J.; Sauve, S.; Mathieu, A.; Guillemette, G.; Leduc, R.; Lavigne, P.; Escher, E. Angiotensin II is Bound to Both Receptors AT_1 and AT_2, Parallel to the Transmembrane Domains and in an Extended Form. *Can. J. Physiol. Pharm.* **2002**, *80*, 418−425.
(19) Printz, M. P.; Nemethy, G.; Bleich, H. Conformational Analysis of Two Cyclic Analogues of Angiotensin: Implications for the Biologically Active Conformation. *Nature* **1972**, *237*, 135−140.
(20) Spear, K. L.; Brown, M. S.; Reinhard, E. J.; McMahon, E. G.; Olins, G. M.; Palomo, M. A.; Patton, D. R. Conformational Restriction of Angiotensin II: Cyclic Analogues Having High Potency. *J. Med. Chem.* **1990**, *33*, 1935−1940.
(21) Sugg, E. E.; Dolan, C. A.; Patchett, A. A.; Chang, R. S. L.; Faust, K. A.; Lotti, V. J. In *Peptides, Chemistry, Structure and Biology, Proceedings of the Eleventh American Peptide Symposium*; Rivier, J. E., Marshall, G. R., Eds.; ESCOM: Leiden, 1990; pp 305−306.
(22) Plucinska, K.; Kataoka, T.; Yodo, M.; Cody, W. L.; He, J. X.; Humblet, C.; Lu, G. H.; Lunney, E.; Major, T. C.; Panek, R. L.; Schelkun, P.; Skeean, R.; Marshall, G. R. Multiple Binding Modes for the Receptor-Bound Conformations of Cyclic AII Agonists. *J. Med. Chem.* **1993**, *36*, 1902−1913.
(23) Schmidt, B.; Lindman, S.; Tong, W.; Lindeberg, G.; Gogoll, A.; Lai, Z.; Thörnwall, M.; Synnergren, B.; Nilsson, A.; Welch, C. J.; Sohtell, M.; Westerlund, C.; Nyberg, F.; Karlén, A.; Hallberg, A. Design, Synthesis, and Biological Activities of Four Angiotensin II Receptor Ligands with γ-Turn Mimetics Replacing Amino Acid Residues 3−5. *J. Med. Chem.* **1997**, *40*, 903−919.
(24) Lindman, S.; Lindeberg, G.; Nyberg, F.; Karlén, A.; Hallberg, A. Comparison of Three γ-Turn Mimetic Scaffolds Incorporated into Angiotensin II. *Bioorg. Med. Chem.* **2000**, *8*, 2375−2383.
(25) Johannesson, P.; Lindeberg, G.; Johansson, A.; Nikiforovich, G. V.; Gogoll, A.; Synnergren, B.; Le Grèves, M.; Nyberg, F.; Karlén, A.; Hallberg, A. Vinyl Sulfide Cyclized Analogues of Angiotensin II with High Affinity and Full Agonist Activity at the AT_1 Receptor. *J. Med. Chem.* **2002**, *45*, 1767−1777.
(26) Samanen, J.; Aiyar, N.; Edwards, R. In *Peptides, Proceedings of the Thirteenth American Peptide Symposium*; Hodges, R. S., Smith, J. A., Eds.; ESCOM: Leiden, 1994; pp 640−642.
(27) Cody, W. L.; He, J. X.; Lunney, E. A.; Humblet, C. C.; Lu, G. H.; Panek, R. L.; Dudley, D. T. Modifications of the C-terminal Dipeptide of Angiotensin II Yielded a Novel Series of Analogues with Type II (AT_2) Receptor Selectivity. *Protein Pept. Lett.* **1996**, *3*, 107−112.
(28) Miura, S.-I.; Karnik, S. S. Angiotensin II Type 1 and Type 2 Receptors Bind Angiotensin II Through Different Types of Epitope Recognition. *J. Hypertens.* **1999**, *17*, 397−404.
(29) Lindman, S.; Lindeberg, G.; Frändberg, P. A.; Nyberg, F.; Karlén, A.; Hallberg, A. Effect of 3−5 Monocyclizations of Angiotensin II and 4-AminoPhe^6-Ang II on AT_2 Receptor Affinity. *Bioorg. Med. Chem.* **2003**, *11*, 2947−2954.
(30) Rosenström, U.; Sköld, C.; Lindeberg, G.; Botros, M.; Nyberg, F.; Karlén, A.; Hallberg, A. A Selective AT_2 Receptor Ligand with a γ−Turn-Like Mimetic Replacing the Amino Acid Residues 4−5 of Angiotensin II. *J. Med. Chem.* **2004**, *47*, 859−870.
(31) Rose, G. D.; Gierasch, L. M.; Smith, J. A. Turns in Peptides and Proteins. *Adv. Protein Chem.* **1985**, *37*, 1−109.
(32) Ball, J. B.; Alewood, P. F. Conformational Constraints: Non-peptide β-Turn Mimics. *J. Mol. Recognit.* **1990**, *3*, 55−64.
(33) Hölzemann, G. Peptide Conformation Mimetics. Part 1. *Kontakte (Darmstadt)* **1991**, 3−12.
(34) Hölzemann, G. Peptide Conformation Mimetics. Part 2. *Kontakte (Darmstadt)* **1991**, 55−63.
(35) Giannis, A.; Kolter, T. Peptidomimetics for Receptor Ligands: Discovery, Development, and Medicinal Perspectives. *Angew. Chem., Int. Ed. Engl.* **1993**, *32*, 1244−1267.
(36) Liskamp, R. M. J. Conformationally Restricted Amino Acids and Dipeptides, (Non)peptidomimetics and Secondary Structure Mimetics. *Recl. Trav. Chim. Pays-Bas* **1994**, *113*, 1−19.
(37) Fairlie, D. P.; West, M. L.; Wong, A. K. Towards Protein Surface Mimetics. *Curr. Med. Chem.* **1998**, *5*, 29−62.
(38) Souers, A. J.; Ellman, J. A. β-Turn Mimetic Library Synthesis: Scaffolds and Applications. *Tetrahedron* **2001**, *57*, 7431−7448.
(39) Burgess, K. Solid-Phase Syntheses of β-Turn Analogues to Mimic or Disrupt Protein−Protein Interactions. *Acc. Chem. Res.* **2001**, *34*, 826−835.
(40) MacDonald, M.; Aubé, J. Approaches to Cyclic Peptide β-Turn Mimics. *Curr. Org. Chem.* **2001**, *5*, 417−438.
(41) Kee, S.; Jois, S. D. S. Design of β-turn Based Therapeutic Agents. *Curr. Pharm. Design* **2003**, *9*, 1209−1224.
(42) Hanessian, S.; McNaughton-Smith, G.; Lombart, H. G.; Lubell, W. D. Design and Synthesis of Conformationally Constrained Amino Acids as Versatile Scaffolds and Peptide Mimetics. *Tetrahedron* **1997**, *53*, 12789−12854 and references therein.
(43) Baures, P. W.; Ojala, W. H.; Costain, W. J.; Ott, M. C.; Pradhan, A.; Gleason, W. B.; Mishra, R. K.; Johnson, R. L. Design, Synthesis, and Dopamine Receptor Modulating Activity of Diketopiperazine Peptidomimetics of L-Prolyl-L-Leucylglycinamide. *J. Med. Chem.* **1997**, *40*, 3594−3600.
(44) Gillespie, P.; Cicariello, J.; Olson, G. L. Conformational Analysis of Dipeptide Mimetics. *Biopolymers* **1997**, *43*, 191−217.
(45) Siddiqui, M. A.; Préville, P.; Tarazi, M.; Warder, S. E.; Eby, P.; Gorseth, E.; Puumala, K.; DiMaio, J. Synthesis of Constrained Bicyclic Dipeptide Mimetics. *Tetrahedron Lett.* **1997**, *38*, 8807−8810.
(46) Subasinghe, N. L.; Khalil, E. M.; Johnson, R. L. Stereospecific Synthesis of 2-substituted Bicyclic Thiazolidine Lactams. *Tetrahedron Lett.* **1997**, *38*, 1317−1320.
(47) Witter, D. J.; Famiglietti, S. J.; Cambier, J. C.; Castelhano, A. L. Design and Synthesis of SH3 Domain Binding Ligands: Modifications of the Consensus Sequence XPpXP. *Bioorg. Med. Chem. Lett.* **1998**, *8*, 3137−3142.
(48) Geyer, A.; Bockelmann, D.; Weissenbach, K.; Fischer, H. Synthesis and Structure of a Hydrophilic β-turn Mimetic. *Tetrahedron Lett.* **1999**, *40*, 477−478.
(49) Khalil, E. M.; Ojala, W. H.; Pradhan, A.; Nair, V. D.; Gleason, W. B.; Mishra, R. K.; Johnson, R. L. Design, Synthesis, and Dopamine Receptor Modulating Activity of Spiro Bicyclic Peptidomimetics of L-Prolyl-L-Leucyl-Glycinamide. *J. Med. Chem.* **1999**, *42*, 628−637.
(50) Khalil, E. M.; Pradhan, A.; Ojala, W. H.; Gleason, W. B.; Mishra, R. K.; Johnson, R. L. Synthesis and Dopamine Receptor Modulating Activity of Substituted Bicyclic Thiazolidine Lactam Peptidomimetics of L-Prolyl-L-Leucyl-Glycinamide. *J. Med. Chem.* **1999**, *42*, 2977−2987.
(51) Qiu, W.; Gu, X.; Soloshonok, V. A.; Carducci, M. D.; Hruby, V. J. Stereoselective Synthesis of Conformationally Constrained Reverse Turn Dipeptide Mimetics. *Tetrahedron Lett.* **2001**, *42*, 145−148.
(52) Gu, X.; Qiu, W.; Ying, J.; Ndungu, J. M.; Hruby, V. J. In *Peptides, The Wave of the Future, Proceedings of the Seventeenth American Peptide Symposium*; Lebl, M., Houghten, R. A., Eds.; American Peptide Society: San Diego, 2001; pp 602−603.
(53) Subasinghe, N. L.; Bontems, R. J.; McIntee, E.; Mishra, R. K.; Johnson, R. L. Bicyclic Thiazolidine Lactam Peptidomimetics of the Dopamine Receptor Modulating Peptide Pro-Leu-Gly-NH_2. *J. Med. Chem.* **1993**, *36*, 2356−2361.
(54) Johannesson, P.; Lindeberg, G.; Tong, W.; Gogoll, A.; Karlén, A.; Hallberg, A. Bicyclic Tripeptide Mimetics with Reverse Turn Inducing Properties. *J. Med. Chem.* **1999**, *42*, 601−608.
(55) Johannesson, P.; Lindeberg, G.; Tong, W.; Gogoll, A.; Synnergren, B.; Nyberg, F.; Karlén, A.; Hallberg, A. Angiotensin II Analogues Encompassing 5,9-and 5,10-Fused Thiazabicycloalkane Tripeptide Mimetics. *J. Med. Chem.* **1999**, *42*, 4524−4537.
(56) Baldwin, J. E.; Lee, V.; Schofield, C. J. Synthesis of a Bicyclic γ-Lactam Dipeptide Analog. *Heterocycles* **1992**, *34*, 903−906.
(57) Ben-Ishai, D. Reaction of Acylamino Acids with Paraformaldehyde. *J. Am. Chem. Soc.* **1957**, *79*, 5736−5738.
(58) Pappo, R.; Allen, D. S., Jr.; Lemieux, R. U.; Johnson, W. S. Osmium Tetroxide-Catalyzed Periodate Oxidation of Olefinic Bonds. *J. Org. Chem.* **1956**, *21*, 478−479.
(59) Carpino, L. A.; Sadat-Aalaee, D.; Guang Chao, H.; DeSelms, R. H. [(9-Fluorenylmethyl)oxy]carbonyl (FMOC) Amino Acid Fluorides. Convienient New Peptide Coupling Reagents Applicable to the FMOC/*tert*-butyl Strategy for Solution and Solid-Phase Syntheses. *J. Am. Chem. Soc.* **1990**, *112*, 9651−9652.
(60) Bertho, J. N.; Loffet, A.; Pinel, C.; Reuther, F.; Sennyey, G. Amino-Acid Fluorides − Their Preparation and Use in Peptide-Synthesis. *Tetrahedron Lett.* **1991**, *32*, 1303−1306.
(61) Kunz, H.; Waldmann, H. Synthesis of the Glycopeptide Partial Sequence A80-A84 of Human Fibroblast Interferon. *Helv. Chim. Acta* **1985**, *68*, 618−622.
(62) Kunz, H.; Dombo, B. Solid-Phase Synthesis of Peptide and Glycopeptide Polymers with Allylic Anchor Groups. *Angew. Chem.* **1988**, *100*, 732−734.
(63) Åkerblom, E. B. Six New Photolabile Linkers for Solid-Phase Synthesis. 2. Coupling of Various Building Blocks and Photolytic Cleavage. *Mol. Divers.* **1998**, *4*, 53−69.
(64) Åkerblom, E. B.; Nygren, A. S.; Agback, K. H. Six New Photolabile Linkers for Solid-Phase Synthesis. 1. Methods of Preparation. *Mol. Divers.* **1998**, *3*, 137−148.
(65) Wokaun, A.; Ernst, R. R. Selective Detection of Multiple Quantum Transitions in NMR by Two-Dimensional Spectroscopy. *Chem. Phys. Lett.* **1977**, *52*, 407−412.

(66) Piantini, U.; Sørensen, O. W.; Ernst, R. R. Multiple Quantum Filters for Elucidating NMR Coupling Networks. *J. Am. Chem. Soc.* **1982**, *104*, 6800−6801.
(67) Shaka, A. J.; Freeman, R. Simplification of NMR Spectra by Filtration through Multiple-Quantum Coherence. *J. Magn. Reson.* **1983**, *51*, 169−173.
(68) Kumar, A.; Ernst, R. R.; Wüthrich, K. A Two-Dimensional Nuclear Overhauser Enhancement (2D NOE) Experiment for the Elucidation of Complete Proton−Proton Cross-Relaxation Networks in Biological Macromolecules. *Biochem. Biophys. Res. Commun.* **1980**, *95*, 1−6.
(69) Bodenhausen, G.; Kogler, H.; Ernst, R. R. Selection of Coherence-Transfer Pathways in NMR Pulse Experiments. *J. Magn. Reson.* **1984**, *58*, 370−388.
(70) Bothner-By, A. A.; Stephens, R. L.; Lee, J.-M.; Warren, C. D.; Jeanloz, R. W. Structure Determination of a Tetrasaccharide: Transient Nuclear Overhauser Effects in the Rotating Frame. *J. Am. Chem. Soc.* **1984**, *106*, 811−813.
(71) Braunschweiler, L.; Ernst, R. R. Coherence Transfer by Isotropic Mixing: Application to Proton Correlation Spectroscopy. *J. Magn. Reson.* **1983**, *53*, 521−528.
(72) Müller, L. Sensitive Enhanced Detection of Weak Nuclei Using Heteronuclear Multiple Quantum Coherence. *J. Am. Chem. Soc.* **1979**, *101*, 4481−4484.
(73) Bax, A.; Subramanian, S. Sensitivity-Enhanced Two-Dimensional Heteronuclear Shift Correlation NMR-Spectroscopy. *J. Magn. Reson.* **1986**, *67*, 565−569.
(74) Parella, T. Pulsed Field Gradients: A New Tool for Routine NMR. *Magn Reson Chem* **1998**, *36*, 467−495.
(75) Still, W. C.; Tempczyk, A.; Hawley, R. C.; Hendrickson, T. Semianalytical Treatment of Solvation for Molecular Mechanics and Dynamics. *J. Am. Chem. Soc.* **1990**, *112*, 6127−6129.
(76) Mohamadi, F.; Richards, N. G. J.; Guida, W. C.; Liskamp, R.; Lipton, M.; Caufield, C.; Chang, G.; Hendrickson, T.; Still, W. C. Macromodel − an Integrated Software System for Modeling Organic and Bioorganic Molecules Using Molecular Mechanics. *J. Comput. Chem.* **1990**, *11*, 440−467.
(77) Dudley, D. T.; Panek, R. L.; Major, T. C.; Lu, G. H.; Bruns, R. F.; Klinkefus, B. A.; Hodges, J. C.; Weishaar, R. E. Subclasses of Angiotensin-II Binding-Sites and Their Functional Significance. *Mol. Pharmacol.* **1990**, *38*, 370−377.
(78) Nielsen, A. H.; Schauser, K.; Winther, H.; Dantzer, V.; Poulsen, K. Angiotensin II Receptors and Renin in the Porcine Uterus: Myometrial AT_2 and Endometrial AT_1 Receptors are Down-Regulated During Gestation. *Clin. Exp. Pharmacol. Physiol.* **1997**, *24*, 309−314.
(79) Belvisi, L.; Bernardi, A.; Manzoni, L.; Potenza, D.; Scolastico, C. Conformational Analysis of Azabicycloalkane Amino Acid Scaffolds as Reverse-Turn Inducer Dipeptide Mimics. *Eur. J. Org. Chem.* **2000**, 2563−2569.
(80) Bouley, R.; Perodin, J.; Plante, H.; Rihakova, L.; Bernier, S. G.; Maletinska, L.; Guillemette, G.; Escher, E. N- and C-terminal Structure−Activity Study of Angiotensin II on the Angiotensin AT_2 Receptor. *Eur. J. Pharmacol.* **1998**, *343*, 323−331.
(81) Gallinat, S.; Busche, S.; Raizada, M. K.; Sumners, C. The Angiotensin II Type 2 Receptor: an Enigma With Multiple Variations. *Am. J. Physiol.* **2000**, *278*, E357-E374.
(82) Knowle, D.; Kurfis, J.; Gavini, N.; Pulakat, L. Role of Asp297 of the AT_2 Receptor in High-Affinity Binding to Different Peptide Ligands. *Peptides* **2001**, *22*, 2145−2149.
(83) Rosenström, U.; Sköld, C.; Lindeberg, G.; Botros, M.; Nyberg, F.; Hallberg, A.; Karlén, A. Synthesis and AT2 receptor-binding properties of angiotensin II analogues. *J. Peptide Res.*, **2004**, in press.
(84) Hodges, J. C.; Hamby, J. M.; Blankley, C. J. Angiotensin II Receptor Binding Inhibitors. *Drugs Future* **1992**, *17*, 575−593 and references therein.

JM049651M